5.2 TORNADO AND TORNADOGENESIS EVENTS SEEN BY THE NOXP, X-BAND, DUAL-POLARIZATION RADAR DURING VORTEX2 2010

Donald W. Burgess *
Cooperative Institute for Mesoscale Meteorological Studies, The University of Oklahoma, and NOAA, NSSL, Norman, OK

Edward R. Mansell
National Severe Storms Laboratory (NSSL)

Christopher M. Schwarz and Blake J. Allen
School of Meteorology, The University of Oklahoma

1. INTRODUCTION

The NOAA (NSSL), X-band, dual-polarimetric radar participated in VORTEX2 (Wurman, et al, 2010), both in 2009 and 2010. During the 2009 field campaign, fewer than average tornadic supercells occurred in the experiment domain. In 2009, NOXP collected data on 4 tornadic supercells [only 1 significantly tornadic (June 5)] and 6 non-tornadic supercells (see Schwarz and Burgess, 2010, this conference, for more information on the 2009 data).

During the VORTEX2 2010 field campaign, more than an average number of supercells occurred in the experiment domain, and NOXP collected a significantly larger data set of 12 tornadic supercells and 22 non-tornadic supercells (Table 1). The tornadic supercell sampled on May 10 was the longest-lasting and most prolific tornado producer of that outbreak. Other significantly tornadic supercells were sampled on May 25, June 7, June 10, and June 13. In addition to the tornadic and non-tornadic supercells, several quasi-linear convective systems (QLCSs) were sampled. Two of the QLCSs (May 24 and June14) produced non-supercell tornadoes while being scanned.

Not much time has elapsed since the end of 2010 data collection, less than 4 months. It has only been possible to do cursory examination of the large data set. Therefore, some of the results shown in Table 1 may change with time. Time has not been available for in-depth analysis to begin on any 2010 data set, particularly with analyses of 2009 data still underway.

This paper will briefly discuss NOXP configuration for 2010 data collection (Section 2), provide summaries of some of the better data collection cases (Section 3), and discuss plans for future analysis of the 2010 data set (Section 4).

*corresponding author address: Don Burgess, NSSL/WRDD/Rm 3933, National Weather Center, 120 David L. Boren Blvd., Norman, OK 73072-7323 email: Donald.Burgess@noaa.gov

Table 1: NOXP Target Storms (2010)

Date	Tornadic Supercell	Non-Tornadic Supercell
May 6		2
May 10	1	1
May 11		1
May 12	2	1
May 15		1
May 17		1
May 19	2	
May 21		1
May 23		1
May 24		1
May 25	1	
May 26		1
May 29		1
June 2		1
June 3		1
June 6		3
June 7	2	
June 9		1
June 10	1	1
June 11	2	
June 12		1
June 13	1	2
Total	**12**	**22**

2. NOXP DATA COLLECTION

NOXP operated as a mesocyclone-scale radar in VORTEX2. It coordinated with 3 other X-band, mesocyclone-scale radars (DOW6, DOW7, and UMXP) to provide low-level coverage of the right flanks of supercells being targeted by armada sensors. In 2010, all four radars had dual-polarization capability and other similarities in their operating characteristics. NOXP configuration parameters for spring 2010 are shown in Table 2.

Table 2: NOXP Parameters

Parameter	Value
Wavelength	3.21 cm
Frequency	9410 MHz
3-dB beamwidth	1.0^o
Peak Power	250 kW
Processor	RPV8
PRF/Nyquist Co-Interval	2500Hz/+/- 19.6 m/s
Max Unambiguous Range	59 km
Gate Length/Spacing	37.5 m/75 m
Azimthal Sampling Rate	0.5^o
Antenna Rotation Rate	29^o/sec
Number of Samples	40

In most storm situations, two of the mesocyclone-scale radars were positioned at relatively close range to the right flank of the target storm (~10-20 km) in order to produce data suitable for dual-Doppler analysis, while the other two radars moved ahead to set up the next dual-Doppler lobe. Each operations day, a decision was made to have the mesocyclone-scale radars operate in 2-minute or 3-minute time syncs, i.e., the interval between volume scan starts. NOXP collected 8 PPI scans for 2-minute syncs (1^o-8^o in 1^o steps) and 12 PPI scans for 3-minute syncs (1^o-12^o in 1^o steps). More information on VORTEX2 radar operation logistics and overall operational plans is at: http://www.vortex2.org/home/.

3. CASE STUDIES

As discussed in Section 1 and shown in Table 1, a large quantity of NOXP data was collected during VORTEX2 2010, and not a lot of time has elapsed since the end of data collection to begin analysis of that data. Therefore, this section will provide only a first look at some of the better data collection days (as judged at this early time). Other data sets not mentioned here might prove as useful as or more useful in satisfying VORTEX2 objectives. Also, time has not been available to properly prepare the data for analysis. Much of the data to be shown below have not had antenna pointing corrections or dealiasing corrections applied to them. None of data have had complete data quality and editing corrections applied to them.

3.1 Case 1: May 10, 2010

May 10 was a regional tornado outbreak day with 54 tornadoes reported within the state of Oklahoma. The strong environmental wind associated with the outbreak produced right-moving supercell storm motions of ~25 m/s. Such speeds required a VORTEX2 mode of data collection not yet used in 2009 or early 2010…the array deployment…a mode where VORTEX2 radars and some other instruments deploy at fixed locations because storms are moving too fast to chase. During the morning and early afternoon of May 10, an array area was defined and radar data collection locations were surveyed. Good data collection sites were deemed important because of the undulating and wooded terrain of east central Oklahoma. Also, the array was purposely placed east of the Oklahoma City metro area because of anticipated difficulties in navigating crowded roads in the metro during rush hour. Figure 1 shows the array location and the distribution of radar echoes at 2130 and 2300 (all times are UTC). Despite appearing at 2130 that the array location might prove useful for data collection, the 2300 depiction clearly shows that the early storms to the southwest of the metro did not move east-northeast as expected, but moved/propagated east, covering only the most southern portion of the fixed array. Radars (including NOXP) and other sensors positioned in the southern portion of the array were able to move south and get ahead of the dominate southern supercell (from Norman to Shawnee, to north of Seminole, to near Henryetta and beyond) as it moved east, but radars and other vehicles deployed in the northern part of the array could not move far enough fast enough to get ahead of the supercell.

NOXP path to get ahead of the Norman supercell is illustrated in Fig.2. After finding a somewhat suitable data collection location north of Wewoka (see Fig. 3), data collection began at 2334. The site was on lower ground with higher terrain in most directions, but was in an open area with no nearby wooded areas. Data were collected on the long-track Tecumseh tornado (the 4th for the cyclic Norman supercell) from 2334 until dissipation at ~2347; a time period after peak intensity (EF3 near Tecumseh and north of Seminole near Seminole Airport). The tornado, although past peak intensity when sampling began, was quite wide (~3.2 km diameter) and still possessed radar-observed, ground-relative wind speeds of ~65 m/s (See Fig. 4). Near 2347, as the Tecumseh tornado was dissipating, a new tornado was produced by the cyclic supercell (#5; the Clearview tornado). The developing Clearview tornado and occluding Tecumseh tornado are both seen in Fig 5. The Clearview tornado was still present at 2359 during the last volume scan of NOXP's deployment. The Clearview tornado was also quite large (up to 3 km diameter), but radar-observed wind speeds were less than those for the Tecumseh tornado (~50 m/s).

3.2 Case 2: June 7, 2010

NOXP first deployed near Lyman, NE about 2330 and collected data on a supercell that produced a

tornado north of Scottsbluff, NE at a range of ~30 km from the radar (data not shown). As the first supercell weakened and moved too far east to sample, a second supercell (behind the first) was targeted (Fig. 6). NOXP moved east through Scottsbluff and set up just west of Minatare at 0110 (see Fig 7). The first scans revealed a relatively strong gust front to the west (max winds ~20 m/s). Very rapid evolution was documented over the next 10 minutes as a low-level rotation signature, strong rear-flank downdraft winds, and a wrapping hook echo all developed. A tornado was indicated by radar at 0120 (see Fig. 8 for a data example at 0125). Maximum radar-observed, ground-relative, tornado winds were ~50 m/s; the same speed as those with the rear-flank gust front winds/mesocyclone winds that wrapped around the south side of the tornado. The same pattern persisted until the deployment ended at 0128. At ~0130 while moving south to get away from the supposed tornado just to the west of the deployment site, a tornado was seen just ahead of the southward moving radar truck. It is not known if the previously-scanned tornado moved to the southeast (as suggested in Fig. 7) or if a new tornado developed to the south of the previous tornado. After stopping to let the tornado pass to the east, NOXP moved south of the high wind area, and began data collection again at 0140. A tornado/high-wind signature was seen until ~0155 (data not shown) as the storm continued to move east-southeast.

3.3 Case 3: June 13, 2010

On this day, a cold front was oriented north-northeast to south-southwest across the northern Texas Panhandle. The cold front intersected an outflow boundary (from overnight convection) across the northern Panhandle. Storms formed early and NOXP first deployed at 1814 ahead of the cold front and near the outflow boundary as a first storm approached the boundary/frontal intersection point. The first storm crossed the outflow boundary, continued to move northeast, and produced a weak supercell that possessed only mid-level rotation.

A second storm approached the intersection point and NOXP repositioned to observe it (Fig. 9). After crossing the boundary, the second storm moved more the east-northeast and slowly gained supercell characteristics. However, only a weak, elongated cyclonic shear region, along a north-south oriented gust front, was seen at low-levels at 2033. At this time, significant cyclonic rotation was confined to storm mid-levels as indicated by KAMA. With time as the storm past just north of the radar site, interesting low-level signatures developed. By 2043 (Fig. 10), a boundary-layer cyclonic circulation couplet was forming, and interesting polarization signatures (apparently different from other tornadic supercells sampled by NOXP) were being observed. A region of strong gradient developed along the shank of the hook echo with a zone of low reflectivity (Zh), high differential reflectivity (Zdr), and very low correlation coefficient (Rhv) adjacent to the more typical hook-shank zone of moderate Zh, moderate Zdr, and high Rhv. One possibility is that the signature results from a strong gradient between updraft with lofted biota and downdraft with rain, but more research will be necessary to confirm the origin of the polarization signature. A second polarization signature was seen toward the tip of the developing knob of the hook echo where weak to moderate Zh, low Zdr, and high Rhv overlap. The nature and origin of this polarization is unknown, and again, more research will be necessary to understand what is occurring with the storm microphysics. Rapid low-level evolution continued with rapidly increasing low-level rotation and a tornado signature that was seen by 2052 (Fig. 11). Remnants of the interesting polarization signatures seen at 2043 were still present, but their contribution to tornadogenesis is difficult to judge at this time. The tornado signature continued to be observed until the end of the deployment at 2102. Maximum radar-observed, ground-relative winds for the tornado were ~50 m/s.

4. PLANS FOR FUTURE ANALYSIS

The first priority for the future will be to continue to perform quality control steps and edit the large volume of data collected in 2010. Because of continuing analysis of 2009 data, it will be several months before detailed analysis of 2010 data can begin.

A robust data set has been collected by NOXP as one of the mobile radars in VORTEX2. However, the premise of the experiment is not to just analyze the data from any one radar or other sensor (although that is the first step), but to integrate all data from the many observational platforms into comprehensive analyses of the target storms. This is a laborious and time consuming exercise, and one that is just beginning. Hopefully, upcoming VORTEX2 meetings will help organize integrated-sensor studies of the many interesting cases, three of which have been illustrated in this paper.

First steps for NOXP data (after quality control and editing) may be dual-Doppler analyses with UMXP for the May 10 case (see Fig. 3 for the location of UMXP and the dual-Doppler baseline). Also, for the same case, MWR-05XP (X-band, phased array; one of the tornado-scale radars; Bluestein et al, 2010) collected a very high time/space resolution tornadogenesis data. These data can be combined with the lower-resolution

NOXP/UMXP dual-Doppler winds to study the tornadogenesis process for the Clearview tornado.

Additional dual-Doppler studies may be possible for other cases. For June 13, it appears a useful dual-Doppler baselines exist with DOW7 for study of that tornadogenesis event. For the June 7 case, dual-Doppler analysis with DOW7 also is possible. Unfortunately, for that case, the radars were relatively close together and baseline between them is short, perhaps limiting the dual-Doppler area just before and during tornadogenesis. Additional instrument data and additional analysis days will undoubtedly be added to current thoughts as further work reveals more about NOXP data and all the other observational platforms.

5. ACKNOWLEDGMENTS

Funding was provided by NOAA/Office of Oceanic and Atmospheric Research under NOAA-University of Oklahoma Cooperative Agreement #NA17RJ1227, U.S. Department of Commerce. Funding was also provided by NSF Grant ATM-0802717. We give special thanks to the NSSL engineers and technicians who prepared and maintained NOXP for VORTEX2 data collection. We also thank Josh Wurman for his hard work as VORTEX2 field radar coordinator. We acknowledge Roger Wakimoto, Nolan Atkins, and their students for damage surveys done for the May 10 and June 7 storms, and Kiel Ortega for his survey for the May 10 storm.

6. REFERENCES

Bluestein, H.B., M.M. French, I. PopStefanija, and R.T. Bluth, 2010: Mobile, phased-array, X-band Doppler radar observations of tornadogenesis in the central U.S. Proceedings, 6th European Conference on Radar Meteorology and Hydrology (ERAD), Sibiu, Romania, 6-10 September 2010, 474-480.

Schwarz, C.M., and D.W. Burgess, 2010: Verification of the origins of rotation in tornadoes experiment, part 2 (VORTEX2): Data from the NOAA (NSSL) X-band dual-polarized radar. 25th Conference on Severe Local Storms, Denver, CO, 11-15 October 2010, P6.1.

Wurman, J., H. Bluestein, D. Burgess, D. Dowell, P. Markowski, Y. Richardson, and L. Wicker, 2010: VORTEX2: The verification of the origins of rotation in tornadoes experiment. Proceedings, 6th European Conference on Radar Meteorology and Hydrology (ERAD), Sibiu, Romania, 6-10 September 2010, 4801-490.

Figure 1. Mosaic radar reflectivity, tornado watches (large rectangles), and warnings (small polygons) for 2130 UTC & 2300 UTC on May 10, 2010. White outline is VORTEX2 array area. (From Iowa Environmental Mesonet)

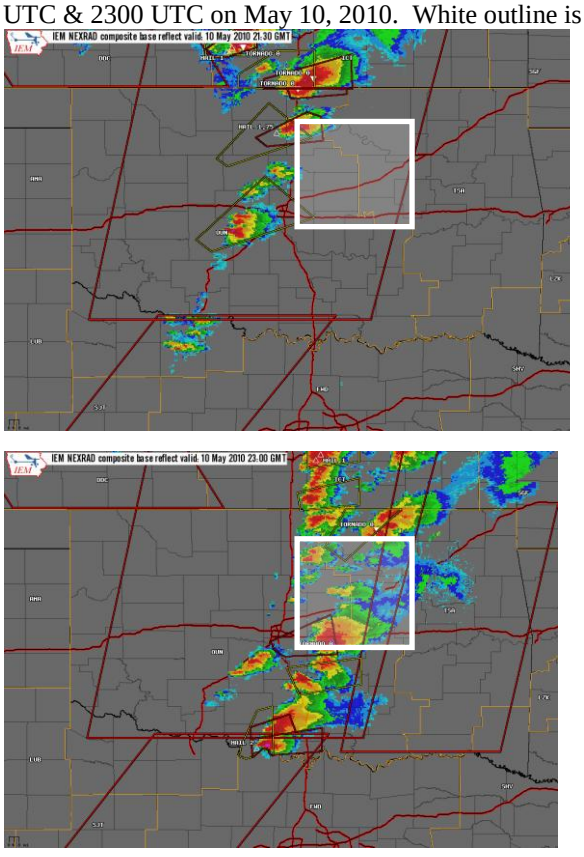

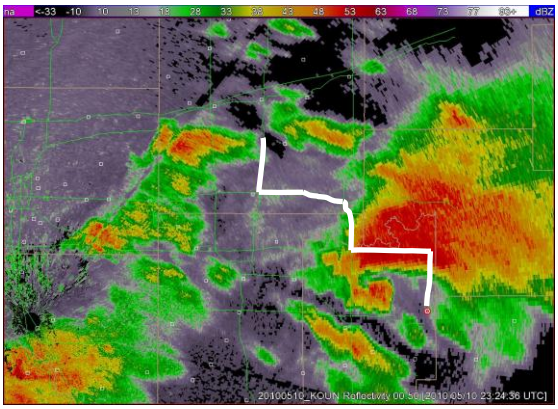

Figure 2. KOUN reflectivity for 0.5° at ~2325 UTC on May 10, 2010. Small circle is location of NOXP . White line segment is path taken by NOXP.

Figure 3. Damage survey for May 10, 2010 near time of NOXP data collection. White outlines are EF0 outlines for Tecumseh (EF3) and Clearview (EF1) tornadoes. Interior green line marks EF2 and greater. Indicated times from radar are in UTC. Locations of NOXP, UMXP and dual-Doppler baseline (yellow line) are shown.

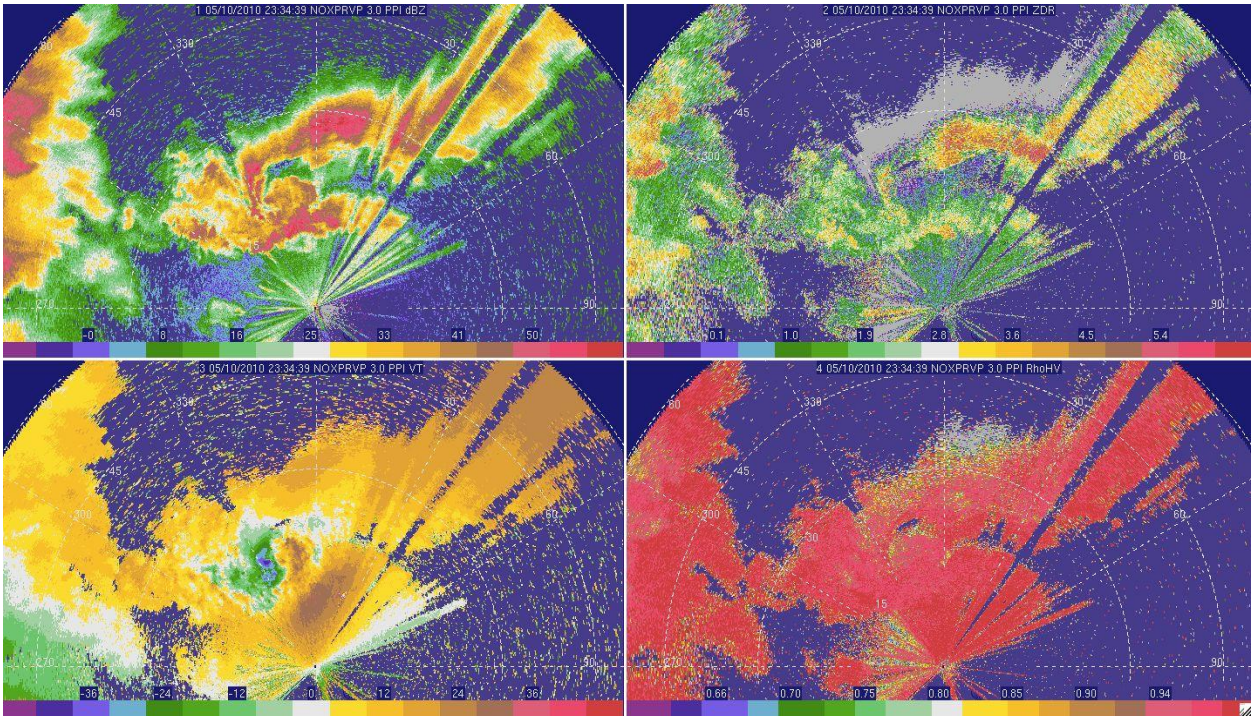

Figure 4. NOXP radar data at ~2335 UTC on May 10, 2010 at 3^0 elevation; reflectivity (upper left), radial velocity (lower left), differential reflectivity (Zdr; upper right), correlation coefficient (Rhv; lower right). Tecumseh tornado signature to the north of the radar.

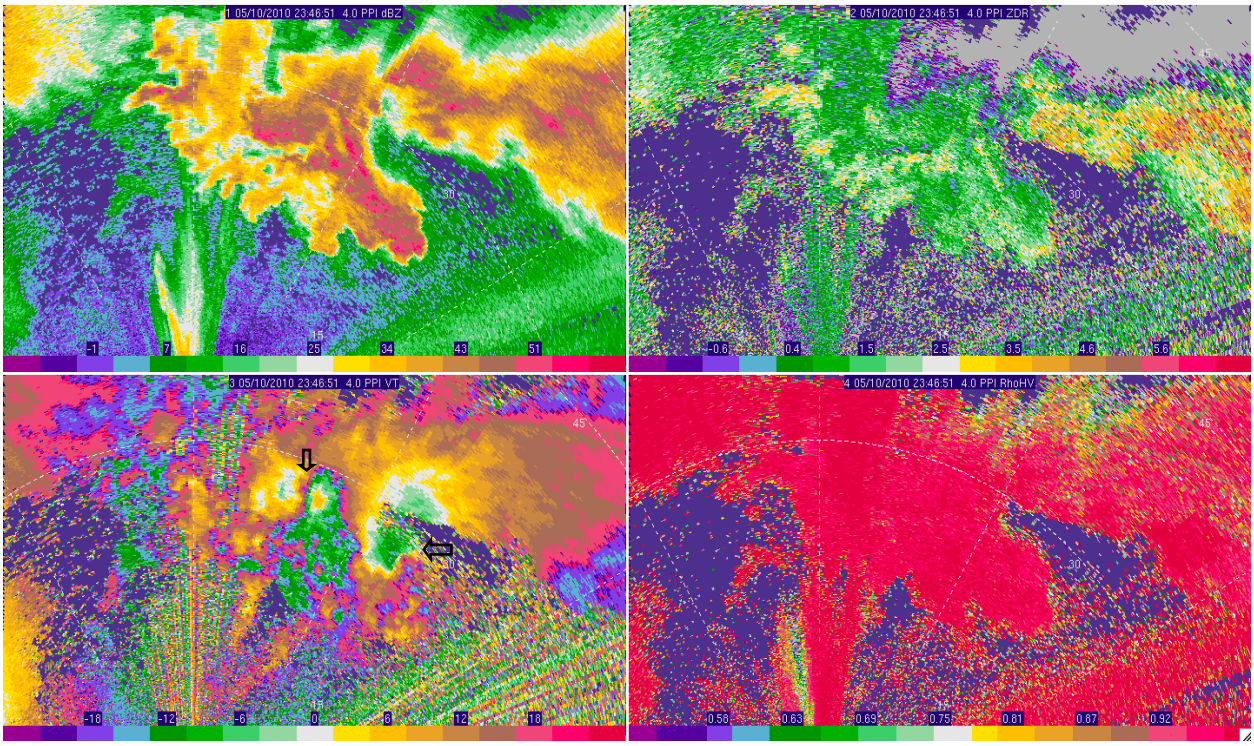

Figure 5. NOXP radar data at ~2347 UTC on May 10, 2010 at 4^0 elevation; reflectivity (upper left), radial velocity (lower left), differential reflectivity (Zdr; upper right), correlation coefficient (Rhv; lower right). Tecumseh tornado (left arrow) and Clearview tornado (right arrow) signatures marked on radial velocity image.

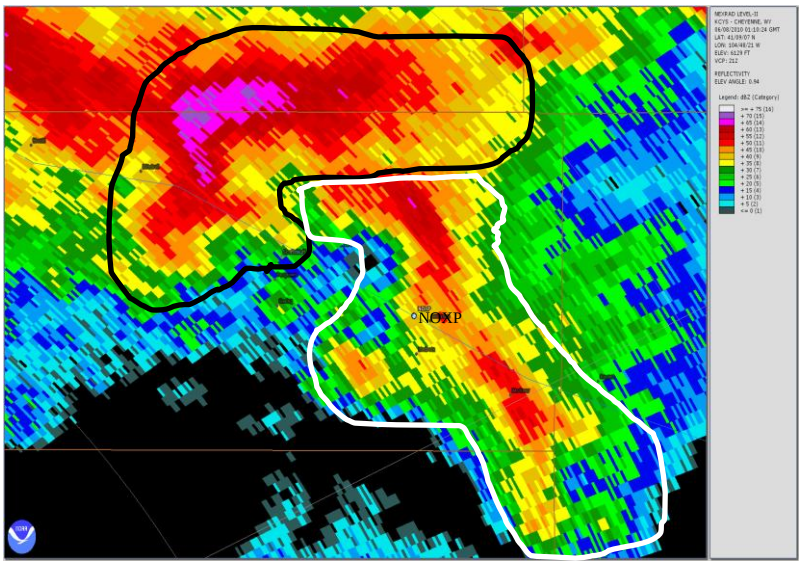

Figure 6. Reflectivity (0.5°) from KCYS at 0110 UTC on June 8 (evening of June 7), 2010. Dark outline is target storm. White outline is left-moving, short line segment that passed ahead of target storm. Location of NOXP marked. Image from NCDC Level2 archive.

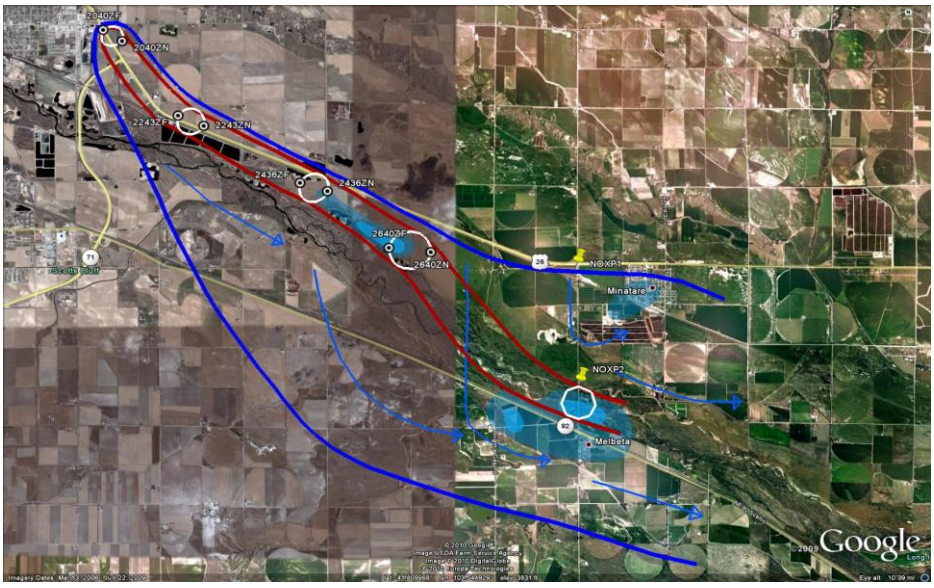

Figure 7. Damage survey of wind (blue outline) and tornado (white circles and red outline) for June 7, 2010. Lighter shading is concentrated area of EF0 damage, darker shading is EF1 damage). NOXP1 is location of data collection; NOXP2 is location of tornado observation.

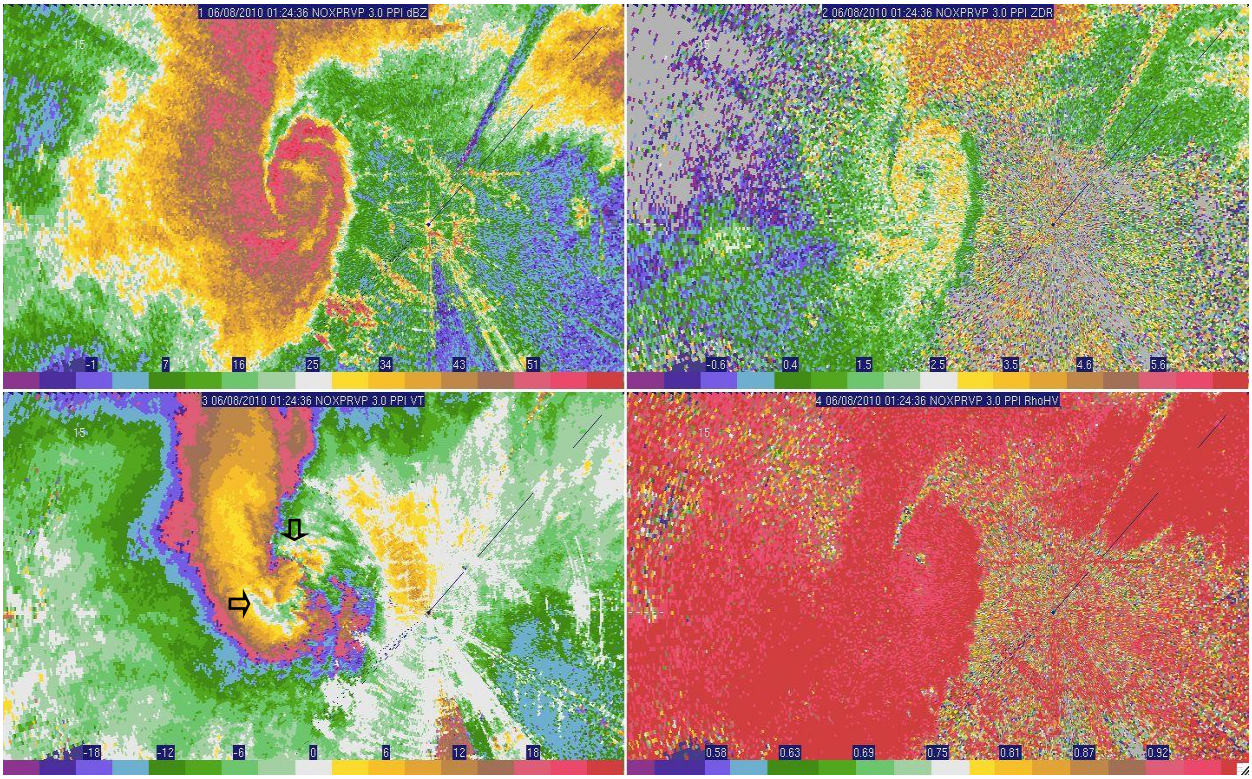

Figure 8. NOXP radar data at ~0125 UTC on June 8, 2010 at 3^0 elevation; reflectivity (upper left), radial velocity (lower left), differential reflectivity (Zdr; upper right), correlation coefficient (Rhv; lower right). Tornado location (upper arrow) and strong rear-flank/mesocyclone winds (lower arrow) marked on radial velocity image.

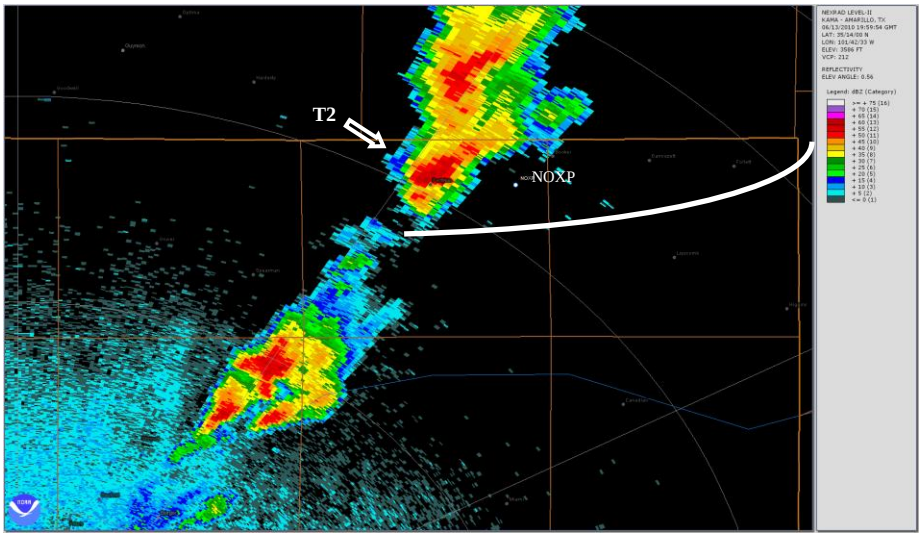

Figure 9. KAMA reflectivity at 0.5^o at 2000 UTC on June 13, 2010. Target storm #2 (T2) marked. Long curved line is approximate location of outflow boundary. Data collection location of NOXP is marked. Image from NCDC Level2 archive.

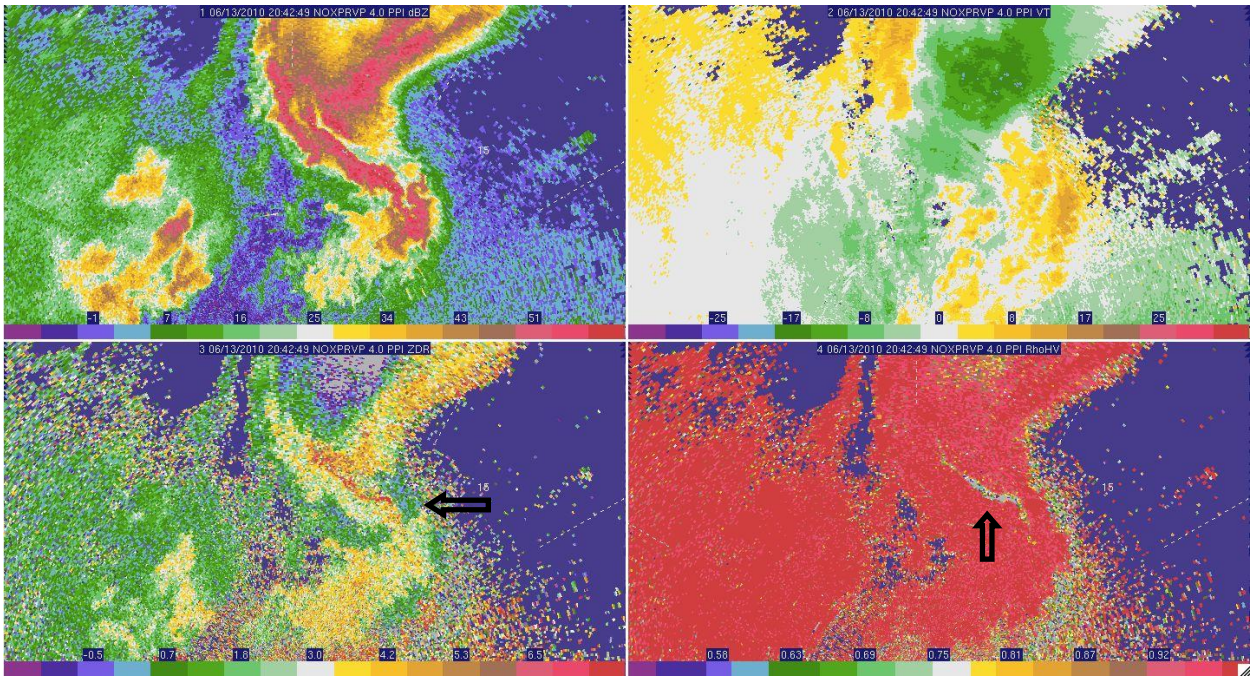

Figure 10. NOXP radar data at ~2043 UTC on June 13, 2010 at 4^{o} elevation; reflectivity (upper left), radial velocity (upper right), differential reflectivity (Zdr; lower left), correlation coefficient (Rhv; lower right). Interesting dual-polarization signatures marked on differential reflectivity and correlation coefficient images (dark arrows).

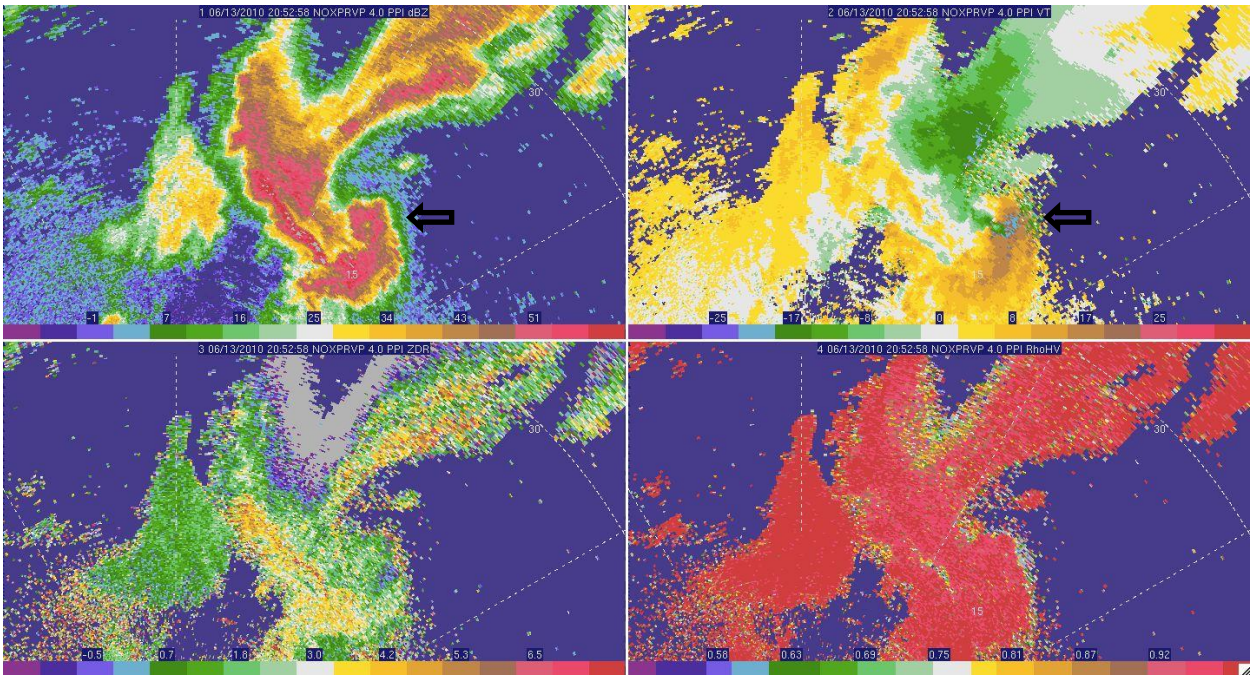

Figure 11. NOXP radar data at ~2053 UTC on June 13, 2010 at 4^{o} elevation; reflectivity (upper left), radial velocity (upper right), differential reflectivity (Zdr; lower left), correlation coefficient (Rhv; lower right). Tornado signature is marked on reflectivity and radial velocity images (dark arrows).